PERSPECTIVE

doi:10.1038/nature11574

Making sense of palaeoclimate sensitivity

PALAEOSENS Project Members*

Many palaeoclimate studies have quantified pre-anthropogenic climate change to calculate climate sensitivity (equilibrium temperature change in response to radiative forcing change), but a lack of consistent methodologies produces a wide range of estimates and hinders comparability of results. Here we present a stricter approach, to improve intercomparison of palaeoclimate sensitivity estimates in a manner compatible with equilibrium projections for future climate change. Over the past 65 million years, this reveals a climate sensitivity (in K W^{-1} m^2) of 0.3–1.9 or 0.6–1.3 at 95% or 68% probability, respectively. The latter implies a warming of 2.2–4.8 K per doubling of atmospheric CO_2, which agrees with IPCC estimates.

Characterizing the complex responses of climate to changes in the radiation budget requires the definition of climate sensitivity: this is the global equilibrium surface temperature response to changes in radiative forcing (an alteration to the balance of incoming and outgoing energy in the Earth–atmosphere system) caused by a doubling of atmospheric CO_2 concentrations. Despite progress in modelling and data acquisition, uncertainties remain regarding the exact value of climate sensitivity and its potential variability through time. The range of climate sensitivities in climate models used for Intergovernmental Panel for Climate Change Assessment Report 4 (IPCC-AR4) is 2.1–4.4 K per CO_2 doubling[1], or a warming of 0.6–1.2 K per W m^{-2} of forcing. Observational studies have not narrowed this range, and the upper limit is particularly difficult to estimate[2].

Large palaeoclimate changes can be used to estimate climate sensitivity on centennial to multi-millennial timescales, when estimates of both global mean temperature and radiative perturbations linked with slow components of the climate system (for example, carbon cycle, land ice) are available (Fig. 1). Here we evaluate published estimates of climate sensitivity from a variety of geological episodes, but find that intercomparison is hindered by differences in the definition of climate sensitivity between studies (Table 1). There is a clear need for consistent definition of which processes are included and excluded in the estimated sensitivity, like the need for strict taxonomy in biology. The definition must agree as closely as possible with that used in modelling studies of past and future climate, while remaining sufficiently pragmatic (operational) to be applicable to studies of different climate states in the geological past.

Here we propose a consistent operational definition for palaeoclimate sensitivity and illustrate how a tighter definition narrows the range of reported estimates. Consistent intercomparison is crucial to detect systematic differences in sensitivity values—for example, due to changing continental configurations, different climate background states, and the types of radiative perturbations considered. These differences may then be evaluated in terms of additional controls on climate sensitivity, such as those arising from plate tectonics, weathering cycles, changes in ocean circulation, non-CO_2 greenhouse gases (GHGs), enhanced water-vapour and cloud feedbacks under warm climate states. Palaeoclimate data allow such investigations across geological episodes with very different climates, both warmer and colder than today. Clarifying the dependence of feedbacks, and therefore climate sensitivity, on the background climate state is a top priority, because it is central to the utility of past climate sensitivity estimates in assessing the credibility of future climate projections[1,3].

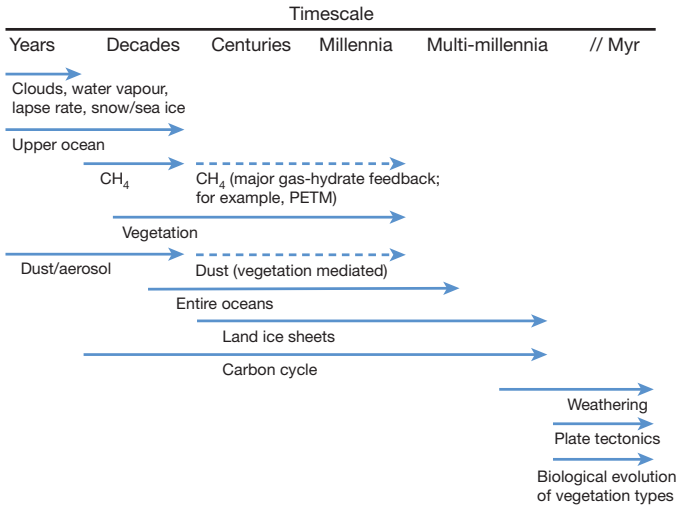

Figure 1 | Typical timescales of different feedbacks relevant to equilibrium climate sensitivity, as discussed in this work. Modified and extended from previous work[98]. Ocean timescales were extended to multi-millennial timescales[99].

Quantifying climate sensitivity

'Equilibrium climate sensitivity' is classically defined as the simulated global mean surface air temperature increase (ΔT, in K) in response to a doubling of atmospheric CO_2, starting from pre-industrial conditions (which corresponds to a radiative perturbation, ΔR, of 3.7 W m^{-2}; refs 1, 3). We introduce the more general definition of the 'climate sensitivity parameter' as the mean surface temperature response to any radiative perturbation ($S = \Delta T/\Delta R$; where ΔT and ΔR are centennial to multi-millennial averages), which facilitates comparisons between studies from different time-slices in Earth history. For brevity, we refer to S as 'climate sensitivity'. In the definition of S, an initial perturbation ΔR_0 leads to a temperature response ΔT_0 following the Stefan–Boltzmann law, which is the temperature-dependent blackbody radiation response. This is often referred to as the Planck response[4], with a value S_0 of about 0.3 K W^{-1} m^2 for the present-day climate[5,6]. The radiative perturbation of the climate system is increased (weakened) by various positive (negative) feedback processes, which operate at a range of different timescales (Fig. 1). Because the net effect of positive feedbacks is found to be greater than that of negative feedbacks, the end result is an increased climate sensitivity relative to the Planck response[4].

*Lists of participants and their affiliations appear at the end of the paper.

Table 1 | Summary of key studies.

Label in Fig. 3	Source	Time window	Explicitly considered forcings	Temperature data used	S and 1σ bounds ($K\,W^{-1}\,m^2$)	Notes
1	Ref. 2	LGM	Various	Various	0.81 ± 0.27 (data); $0.81^{+0.4}_{-0.27}$ (models)	LGM compilation based on ref. 15
2	Ref. 6	LGM	GHG (CO_2, CH_4, N_2O), LI, AE, VG	$\Delta T_{global} = -5.8 \pm 1.4$ K; GLAMAP extrapolated with model[82]	$0.72^{+0.33}_{-0.23}$	Scaling factor (0.85) for smaller S at LGM compared to $2 \times CO_2$ (refs 12, 16)
3	Ref. 86	LGM	GHG (CO_2, CH_4), LI, AE, VG	CLIMAP and $\Delta T_{aa\&gld}$	0.80 ± 0.14	Value after authors' suggested correction of CLIMAP temperatures
4	Ref. 79	LGM	GHG (CO_2, CH_4), LI, AE, VG	MARGO[81] SST based $\Delta T = -3.0^{+1.3}_{-0.7}$ K	$0.62^{+0.08}_{-0.12}$	Model-based global estimate
5	Ref. 76	GC	GHG (CO_2, CH_4)	ΔT_{trop}	1.1 ± 0.05	Author's linear regression case. Value based on single-site tropical SST, and representation of global changes will be more uncertain
6	Ref. 74	GC	GHG (CO_2, CH_4), LI, AE	ΔT_{aa} (with $1.5\times$ polar amplification)	0.88 ± 0.13	Author used a single value for polar amplification. If $2\times$ were used[52], then the central estimate is closer to 0.7
7	Ref. 52	GC	GHG (CO_2, CH_4, N_2O), LI	ΔT_{aa} (with $2\times$ polar amplification)	0.75 ± 0.13	Authors used a single value for polar amplification. If $1.5\times$ were used[74], then the central estimate becomes 1.0
8	Ref. 52	GC	GHG (CO_2, CH_4, N_2O)	ΔT_{aa} (with $2\times$ polar amplification)	1.5 ± 0.25	Authors used a single value for polar amplification. If $1.5\times$ were used[74], then the central estimate becomes 2.0
23–32	This work, based on ref. 6	GC (<800 kyr ago)	GHG (CO_2, CH_4, N_2O), LI, AE, VG	ΔT_{NH} = model-based deconvolution of benthic $\delta^{18}O$ (ref. 51), scaled to global ΔT using a NH polar amplification on land of 2.75 ± 0.25	0.66 ± 0.22 to 2.26 ± 0.78	This covers the range of $S_{[GHG,X]}$ given in Table 2
9	Ref. 85	GC	GHG (CO_2, CH_4, N_2O), LI	ΔT_{aa} (with $2\times$ polar amplification) and $1.5 \times \Delta T_{ds}$	0.75 ± 0.13	Authors used a single value for polar amplification. If $1.5\times$ were used[73], then the central estimate becomes 1.0
10	Ref. 39	GC	GHG (CO_2, CH_4, N_2O), LI, AE	36-record global SST synthesis along with $\Delta T_{aa\&gld}$.	$0.85^{+0.25}_{-0.2}$	Polar amplification diagnosed, not imposed. Estimates made both in a spatially explicit sense and as direct global means
11	Ref. 39	GC	GHG (CO_2, CH_4, N_2O), LI	36-record global SST synthesis along with $\Delta T_{aa\&gld}$.	1.05 ± 0.25	As above
12	Ref. 87	Early to Middle Pliocene (4.2–3.3 Myr ago)	CO_2, ESS	Using model-based ΔT for Middle and Early Pliocene of 2.4–2.9 °C and 4 °C. ΔCO_2 alkenone	1.92 ± 0.14 to 2.35 ± 0.18 (3.3 Myr ago); 2.60 ± 0.19 (4.2 Myr ago)	Forcing in ref. 44; temperature in ref. 87. Both derived in global sense from model experiments
13	Ref. 65	Miocene optimum to present day	Slow feedbacks	Deconvolution of benthic $\delta^{18}O$ (ref. 63)	$0.78 \pm 10\%$	$f = 0.71$, $\beta = 5.35$, $\gamma = 1.3$. Details in Supplementary Information
14	This work (compilation)	Eocene–Oligocene transition (~34 Myr ago)	CO_2. ESS (in the sense of ref. 44)	Model-based ΔT, with range of CO_2 values	$1.72^{+0.9}_{-0.54}$	Details in Supplementary Information
15	This work (compilation)	Late Eocene versus present	CO_2. ESS (in the sense of ref. 44)	Model-based ΔT, with range of CO_2 values	$1.82^{+0.26}_{-0.49}$	Details in Supplementary Information
16	Ref. 78	Middle Eocene Climatic Optimum (~40 Myr ago)	CO_2. Ice-free world. Event study (not affected by plate tectonics and evolution effects)	ΔT_{ds} (2 records) and ΔT_{mg} (7 records). ΔCO_2 from alkenones	0.95 ± 0.3	500 kyr timescale. $\Delta T_{ds} = \Delta T_{mg}$. Temperatures from subtropics to high latitudes; no tropical data. Hence biased to high-latitude sensitivity
17	Ref. 78	Mid to Late Eocene transition (41–35 Myr ago)	CO_2. Largely ice-free world. Event study (not affected by plate tectonics and evolution effects)	ΔT_{ds} (ref. 71) and ΔT_{mg}. ΔCO_2 = difference mid Eocene alkenone and late Eocene $\delta^{11}B$	0.95 ± 0.3	Multi-million-year timescale. Adding uncertainty of ± 1 °C to ΔT would enhance 1σ limits to $\pm 0.45\ K\,W^{-1}\,m^2$
18	Ref. 88	Early Eocene (~55–50 Myr ago)	CO_2. Ice-free world. (potential influences of plate tectonics and biological evolution not considered)	ΔT_{mg} (refs 89–91). ΔCO_2 based on modelling[91] marine organic carbon isotope fractionation[92] and soil nodules[93]	0.65 ± 0.25	Central value recalculated in ref. 94. Note ref. 89 underestimated tropical SST
19	This work (compilation)	PETM (~56 Myr ago)	CO_2. Ice-free world. Event study (not affected by plate tectonics and evolution effects)	ΔT_{ds} (>6 records) and ΔT_{mg} (>11 records; equatorial to polar). ΔCO_2 based on deep ocean carbonate chemistry[72, 95]	1.0–1.8	Details in Supplementary Information. Assumes all warming due to C input, and range of background CO_2 and C-injection scenarios. $\Delta T_{ds} = \Delta T_{mg}$. Total range of S is 0.7–2.2 $K\,W^{-1}\,m^2$.

Table 1 | Continued

Label in Fig. 3	Source	Time window	Explicitly considered forcings	Temperature data used	S and 1σ bounds ($K W^{-1} m^2$)	Notes
20	Ref. 96	Cretaceous and early Palaeogene	CO_2. Largely ice-free world. (potential influences of plate tectonics and biological evolution not considered)		1	Recalculated in ref. 94. No uncertainty range was reported, nor salient details for assessment. Figure 3b, c assumes ±25%
21	Ref. 94	Cretaceous and early Palaeogene	CO_2. Largely ice-free world. ESS in the sense of ref. 44	ΔT after refs 52, 71. ΔCO_2 based on ref. 60.	>0.8	No uncertainty range reported. This is a lower bound estimate only
22	Ref. 97	Phanerozoic	CO_2. Ice-free situation. (Potential influences of plate tectonics and biological evolution not considered).	ΔT_{mg}, ΔCO_2 based on GEOCARBSULF	0.8–1.08	Model-based with extensive uncertainty analysis

These studies have empirically determined S for the Pleistocene and some deep-time periods from comparison between data-derived time series for temperature and for radiative change. Comparison of results between studies is greatly hindered by the different 'versions' of S used, as related to different notions of which processes should be explicitly accounted for, and by the different approaches taken to approximate global mean surface temperature. All uncertainties are as originally reported, but shown here at the level equivalent to 1σ, estimated where necessary by dividing total range values by a factor of 2. All values for S are reported in $K W^{-1} m^2$, where necessary after transformation using 3.7 $W m^{-2}$ per doubling of CO_2, bearing in mind the caveats for this at high CO_2 concentrations as elaborated in the main text. GC, glacial cycles; LGM, Last Glacial Maximum; PETM, Palaeocene/Eocene thermal maximum; SST, sea surface temperature. See main text for details of forcings. Subscripts: aa, Antarctica; gld, Greenland; trop, tropical; ds, deep sea; global, global mean; mg, Mg/Ca; NH, Northern Hemisphere.

We emphasize that all feedbacks, and thus the calculated climate sensitivity, may depend in a—largely unknown—nonlinear manner on the state of the system before perturbation (the 'background climate state') and on the type of forcing[7–15]. The relationship of S with background climate state differs among climate models[12,16–18]. A suggestion of state dependence is also found in a data comparison (Table 2)[6], where climate sensitivity for the past 800,000 years (800 kyr) shows substantial fluctuations through time (Fig. 2). In contrast, its values for the Last Glacial Maximum (LGM) alone occupy only the lower half of that range (Fig. 2). That evaluation also suggests that the relationship of S with the general climate state may not be simple.

'Fast' versus 'slow' processes

Climate sensitivity depends on processes that operate on many different timescales, from seconds to millions of years, due to both direct response to external radiative forcing, and internal feedback processes (Fig. 1). Hence, the timescale over which climate sensitivity is considered is critical. An operationally pragmatic decision is needed to categorize a process as 'slow' or 'fast', depending on the timescale of interest, the resolution of the (palaeo-)records considered and the character of changes therein[19]. If a process results in temperature changes that reach steady state slower than the timescale of the underlying radiative perturbation, then it is considered 'slow'; if it is faster or coincident, then it is 'fast'. Present-day atmospheric GHG concentrations and the radiative perturbation due to anthropogenic emissions increase much faster than observed for any natural process within the Cenozoic era[20–22].

For the present, the relevant timescale for distinguishing between fast and slow processes can be taken as 100 yr (ref. 23). Ocean heat uptake plays out over multiple centuries. Combined with further 'slow' processes, it causes climate change over the next few decades to centuries to be dominated by the so-called 'transient climate response' to radiative changes that result from changing GHG concentrations and aerosols[5,19,24]. After about 100 yr, this transient climate response is thought to amount to roughly two-thirds of the equilibrium (see below) climate sensitivity[5,25]. Climate models account for the fast feedbacks from changes in water-vapour content, lapse rate, cloud cover, snow and sea-ice albedo[26], and the resulting response is often referred to as the 'fast-feedback' or 'Charney' sensitivity[23]. To approximate the 'equilibrium' value of that climate sensitivity, accounting for ocean heat uptake and further slow processes, models might be run over centuries with all the associated computational difficulties[27–30], or alternative approaches may be used that exploit the energy balance of the system for known forcing or extrapolation to equilibrium[31].

In palaeoclimate studies, an operational distinction has emerged to distinguish 'fast' and 'slow' processes relative to the timescales of temperature responses measured in palaeodata, where 'fast' is taken to apply to processes up to centennial scales, and 'slow' to processes with timescales close to millennial or longer. Thus, changes in natural GHG concentrations are dominated by 'slow' feedbacks related to global biogeochemical cycles (Fig. 1). Similarly slow are the radiative influences of albedo feedbacks that are dominated by centennial-scale or longer changes in global vegetation cover and global ice area/volume (continental ice sheets) (Fig. 1).

Table 2 | Common permutations of S that may be encountered in palaeostudies

Label in Fig. 3	S definition	Explicitly considered radiative perturbation	Period in which it is practical to use the definition	$S \pm 1\sigma$ for 800 kyr ($K W^{-1} m^2$)	$S \pm 1\sigma$ for LGM ($K W^{-1} m^2$)	S for Pliocene ($K W^{-1} m^2$)
23	$S_{[CO2]}$	$\Delta R_{[CO2]}$	All (especially pre-35 Myr ago when LI ≈ 0)	3.08 ± 0.96	2.63 ± 0.57	1.2
24	$S_{[CO2, LI]}$	$\Delta R_{[CO2, LI]}$	<35 Myr ago	1.07 ± 0.40	0.95 ± 0.22	0.97
25	$S_{[CO2, LI, VG]}$	$\Delta R_{[CO2, LI, VG]}$	<35 Myr ago	0.86 ± 0.27	0.80 ± 0.19	0.82
26	$S_{[CO2, LI, AE]}$	$\Delta R_{[CO2, LI, AE]}$	<35 Myr ago, but mainly <800 kyr ago	0.90 ± 0.42	0.72 ± 0.18	
27	$S_{[CO2, LI, AE, VG]}$	$\Delta R_{[CO2, LI, AE, VG]}$	<35 Myr ago, but mainly <800 kyr ago	0.75 ± 0.29	0.63 ± 0.15	
28	$S_{[GHG]}$	$\Delta R_{[GHG]}$	<800 kyr ago	2.32 ± 0.76	1.97 ± 0.41	
29	$S_{[GHG, LI]}$	$\Delta R_{[GHG, LI]}$	<800 kyr ago	0.96 ± 0.36	0.85 ± 0.19	
30	$S_{[GHG, LI, VG]}$	$\Delta R_{[GHG, LI, VG]}$	<800 kyr ago	0.78 ± 0.23	0.73 ± 0.16	
31	$S_{[GHG, LI, AE]}$	$\Delta R_{[GHG, LI, AE]}$	<800 kyr ago	0.82 ± 0.36	0.66 ± 0.16	
32	$S_{[GHG, LI, AE, VG]}$	$\Delta R_{[GHG, LI, AE, VG]}$	<800 kyr ago	0.68 ± 0.24	0.58 ± 0.14	

S (second column) is presented with a subscript that identifies the explicitly considered radiative perturbations ΔR (third column, same subscripts as for S); all other processes are implicitly resolved as feedbacks within S. The period in which the various definitions of S are practical is determined by the availability of data for the explicitly considered processes. Subscript CO2 indicates the radiative impact of atmospheric CO_2 concentration changes; LI represents the radiative impact of global land ice-volume changes; VG stands for the radiative impact of global vegetation cover changes; AE indicates the radiative impact of aerosol changes; GHG stands for the impact of changes in all non-water natural greenhouse gases (notably CO_2, CH_4 and N_2O). Columns 5 and 6 give calculated values for all suggested permutations of S for the past 800 kyr or the LGM, respectively, based on a previous data compilation[6]. Mean values of all $S_{[X]}$ for the LGM are about 13% smaller than for the whole 800 kyr, but lie well within the given uncertainties. This offset illustrates the state-dependence of S (see Supplementary Information). Column 7 gives examples for the Pliocene[13,44]; Fig. 3b, c assumes ±25% uncertainty in these. In these values the effects of orographic changes have been taken into account (see Supplementary Information section B2).

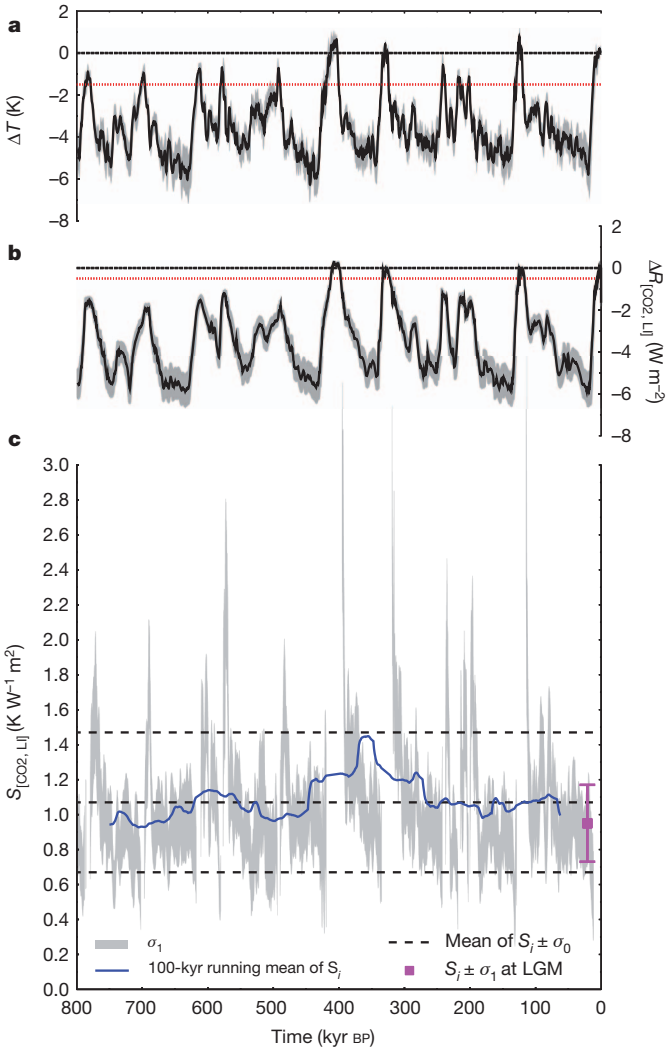

Figure 2 | Illustration of variability of climate sensitivity using a calculation of $S_{[CO2,LI]}$, as defined in this work, for the past 800 kyr. **a**, Changes in global temperature. **b**, Changes in radiative forcing due to changes in CO_2 and surface albedo due to land ice. **c**, Calculated $S_{[CO2,LI]}$, which is only considered robust and calculated when $\Delta T < -1.5$ K and $\Delta R_{[CO2,LI]} < -0.5$ W m^{-2}, as indicated by the dotted red lines in **a** and **b**. In **c**, mean of $S_i \pm \sigma_0$ (dashed black lines indicate σ_0, the uncertainty of averaging) and 100-kyr running mean (blue line) are shown. Magenta marker in **c** denotes $S_i \pm \sigma_1$ for the LGM only (23–19 kyr ago) (σ_1 is the square root of the sum of squares of individual uncertainties connected with different processes contributing to S_i). The grey areas in **a**–**c** denote σ_1 (standard deviation) uncertainties of S_i for single points in time (points themselves are omitted for clarity). Details of data and the definition of the calculated uncertainties presented in this figure are available in Supplementary Information. In **a** and **b**, the dashed black lines indicate the preindustrial reference case ($\Delta T = 0$ K, $\Delta R_{[CO2,LI]} = 0$ W m^{-2}).

Other processes clearly have both fast and slow components. For example, palaeorecords of atmospheric dust deposition imply important aerosol variations on decadal to astronomical (orbital) timescales[32–36], reflecting both slow controlling processes related to ice-volume and land-surface changes, and fast processes related to changes in atmospheric circulation. A further complication arises from the lack of adequate global atmospheric dust data for any geological episode except the LGM[37,38], even though that is essential because the spatial distribution of dust in the atmosphere tends to be inhomogeneous and because temporal variations in some locations tend to take place over several orders of magnitude[32–36]. Moreover, palaeoclimate models generally struggle to account for aerosols, with experiments neither prescribing nor implicitly resolving aerosol influences. So far, understanding of aerosol/dust feedbacks remains weak and in need of improvements in both data coverage and process modelling, especially because dust forcing may account for some 20% of the glacial–interglacial change in the radiative budget[6,39].

So for comparison of results between studies, it is most effective to consider only the classical 'Charney' water-vapour, cloud, lapse rate, and snow and sea-ice feedbacks[23] as 'fast', and all other feedbacks as 'slow'. In addition, results from palaeoclimate sensitivity studies generally do not address the transient climate response that dominates present-day changes, but capture a more complete longer-term system response comparable with equilibrium climate sensitivity in climate models.

Forcing and slow feedbacks

The external drivers of past natural climate changes mainly resulted from changes in solar luminosity over time[40], from temporal and spatial variations in insolation due to changes in astronomical parameters[41–43], from changes in continental configurations[14,44], and from geological processes that directly affect the carbon cycle (for example, volcanic outgassing). However, the complete Earth system response to such forcings as recorded by palaeodata cannot be immediately deduced from the (equilibrium) 'fast feedback' sensitivity of climate models, because of the inclusion of slow feedback contributions. When estimating climate sensitivity from palaeodata, agreement is therefore needed about which of the slower feedback processes are viewed as feedbacks (implicitly accounted for in S), and which are best considered as radiative forcings (explicitly accounted for in ΔR).

We employ an operational distinction[31,45] in which a process is considered as a radiative forcing if its radiative influence is not changing with temperature on the timescale considered, and as a feedback if its impact on the radiation balance is affected by temperature changes on that timescale. For example, the radiative impacts of GHG changes over the past 800 kyr may be derived from concentration measurements of CO_2, CH_4 and N_2O in ice cores[46–48], and the radiative impacts of land-ice albedo changes may be calculated from continental ice-sheet estimates, mainly based on sea-level records[49–51]. Thus, the impacts of these slow feedbacks can be explicitly accounted for before climate sensitivity is calculated. This leaves only fast feedbacks to be considered implicitly in the calculated climate sensitivity, which so approximates the (equilibrium) 'Charney' sensitivity from modelling studies[6,39,52].

Operational challenges

All palaeoclimate sensitivity studies are affected by limitations of data availability. Below we discuss such limitations to reconstructions of forcings and feedbacks, and of global surface temperature responses. First, however, we re-iterate a critical caveat, namely that the climate response depends to some degree on the type of forcing (for example, shortwave versus longwave, surface versus top-of-atmosphere, and local versus global). The various radiative forcings with similar absolute magnitudes have different spatial distributions and physics, so that the concept of global mean radiative forcing is a simplification that introduces some (difficult to quantify) uncertainty.

Astronomical (orbital) forcing is a key driver of climate change. In global annual mean calculations of radiative change, astronomical forcing is very small and often ignored[39,52]. Although this obscures its importance, mainly concerning seasonal changes in the spatial distribution of insolation over the planet[41,42,53–55], we propose that the contribution of the astronomical forcing to ΔR may be neglected initially. When other components of the system respond to the seasonal aspects of forcing, such as Quaternary ice-sheet variations, these may be accounted for as forcings themselves.

GHG concentrations from ice cores are not available for times before 800 kyr ago, when CO_2 levels instead have to be estimated from indirect methods. These employ physico-chemical or biological processes that depend on CO_2 concentrations, such as the abundance of stomata on fossil leaves[56], fractionation of stable carbon isotopes by marine phytoplankton[57], boron speciation and isotopic fractionation in sea water as a function of pH and preserved in biogenic calcite[58], and the stability fields of minerals precipitated from waters in contact with the atmosphere[59].

Considerable uncertainties remain in such reconstructions, but improvements are continually made to the methods, their temporal coverage and their mutual consistency[60]. Recent work has synthesized a high-resolution CO_2 record for the past 20 million years (Myr; ref. 61), but new data and updated syntheses remain essential, particularly for warmer climate states. Also, proxies are needed for reconstruction of CH_4 and N_2O concentrations in periods pre-dating the ice-core records[62].

Regarding the assessment of land-ice albedo changes, good methods exist for the generation of continuous centennial- to millennial-scale sea-level (ice-volume) records over the past 500 kyr (refs 49–51), but such detailed information remains scarce for older periods. A model-based deconvolution of deep-sea stable oxygen isotope records into their ice-volume and deep-sea temperature components[51] was recently extended to 35 Myr ago[63], but urgently requires independent validation, especially to address uncertainties about the volume-to-area relationships that would be different for incipient ice sheets than for mature ice sheets[64,65]. Before 35 Myr ago, there is thought to have been (virtually) no significant land-ice volume[66], but this does not exclude the potential existence of major semi-permanent snow/ice-fields[67,68], and there remain questions whether these would constitute 'fast' (snow) or 'slow' (land-ice) feedbacks. The contribution of the sea-ice albedo feedback also remains uncertain, with little quantitative information beyond the LGM.

Similar examples of uncertainties and limited data availability could be listed for all feedbacks. However, a 'deep-time' (before 1 Myr ago) geological perspective must be maintained because it offers access to the nearest natural approximations of the current rate and magnitude of GHG emissions[69,70], and because only ancient records provide insight into climate states globally warmer than the present. Given that no past perturbation will ever present a perfect analogue for the continuing anthropogenic perturbation, it may be more useful to consider past warm climate states as test-beds for evaluating processes and responses, and for challenging/validating model simulations of those past climate states. Such data–model comparisons will drive model skill and understanding of processes, improving confidence in future multi-century projections. For such an approach, palaeostudies may minimize the impacts of very long-term influences on climate sensitivity (for example, due to changes in orography, or biological evolution of vegetation) through a focus on highly resolved documentation of specific perturbations that are superimposed upon different long-term background climate states. An example is the pronounced transient global warming and carbon-cycle perturbation during the Palaeocene/Eocene thermal maximum (PETM) anomaly[71,72], which punctuated an already warm climate state[73]. Note that deep-time case studies need to consider one further complication, namely that the radiative forcing per CO_2 doubling may be about 3.7 W m^{-2} when starting from pre-industrial concentrations, but increases at higher CO_2 levels[11]. Data-led studies may help with a first-order documentation of this dependence. Calculation of S from CO_2 and temperature measurements using a constant 3.7 W m^{-2} per CO_2 doubling would (knowingly) overestimate S for high-CO_2 episodes. The difference with other, identically defined, S values for different climate background states may then be used to assess any deviation from 3.7 W m^{-2} per CO_2 doubling.

Regarding the reconstruction of past global surface temperature responses (that is, ΔT in equation (1) below), again much remains to be improved. Most work to date (see Table 1) relies on one or more of the following: polar temperature variations from Antarctic ice cores (since 800 kyr ago) with a multiplicative correction for 'polar amplification' (usually estimated at 1.5–2.0; refs 74, 75); deep-sea temperature variations from marine sediment-core data with a correction for the ratio between global surface temperature and deep-sea temperature changes (often estimated at 1.5); single-site sea surface temperature (SST) records from marine sediment cores; or compilations of SST data of varying geographic coverage from marine sediment cores[6,39,52,76–78]. So far, few studies have included terrestrial temperature proxy records other than those from ice cores[79], yet better control on land-surface data is crucial because of seasonal and land-sea contrasts. Continued development is needed of independently validated (multi-proxy) and spatially representative (global) data sets of high temporal resolution relative to the climate perturbations studied.

Uncertainties in individual reconstructions of temperature change may in exceptional cases be reported to ±0.5 K, but more comprehensive uncertainty assessments normally find them to be larger[80,81]. Compilation of such records to determine changes in global mean surface temperature involves the propagation of further assumptions/uncertainties, for example due to interpolation from limited spatial coverage, and the end result is unlikely to be constrained within narrower limits than ±1 K even for well-studied intervals. Finally, comparisons between independent reconstructions for the same episode reveal 'hidden' uncertainties due to differences between each study's methodological choices, uncertainty determination, and data-quality criteria, which are hard to quantify and often poorly elucidated. Take the LGM for example, which for temperature is among the best-studied intervals. The MARGO compilation[81] inferred a global SST reduction of –1.9 ± 1.8 K relative to the present. Another spatially explicit study[79] used that range to infer a global mean surface air temperature anomaly of $-3^{+1.3}_{-0.7}$K. The latter contrasts with a previous estimate of −5.8 ± 1.4 K (ref. 82), which is consistent with tropical (30° S to 30° N) SST anomalies of −2.7 ± 1.4 K (ref. 83). However, that tropical range itself is also contested; the MARGO[81] study suggested such cooling in the Atlantic Ocean, but less in the tropics of the Indian and Pacific Oceans (giving a global tropical cooling of only −1.7 ± 1.0 K). Clearly, even a well-studied interval gives rise to a range of estimates for temperature, and therefore for climate sensitivity.

It is evident that progress in quantifying palaeoclimate sensitivity will not only rely on a common concept and terminology that allows like-for-like comparisons (see below); it will also rely on an objective, transparent and hence reproducible discussion in each study of the assumptions and uncertainties that affect the values determined for change in both temperature and radiative forcing.

A way forward

Here we propose a new terminology to help palaeoclimate sensitivity studies adopt common concepts and approaches, and thus improve the potential for like-for-like comparisons between studies. First we outline how our concept of 'equilibrium' S for palaeo-studies relates to 'equilibrium' S for modern studies. Then, we present a notation system that is primarily of value to data-based palaeo studies to clarify which slow feedbacks are explicitly accounted for. We finish with an application of the new framework, calculating climate sensitivity from a representative selection of palaeoclimate sensitivity estimates over the past 65 Myr, with a fair balance of climates warmer than the present to those colder than the present.

When the ΔT response to an applied GHG radiative forcing ΔR is small relative to 'pre-perturbation' reference temperature, the 'equilibrium' climate sensitivity S^a (where a indicates *actuo*, for present-day) takes the form (see, for example, refs 4, 84):

$$S^a = \frac{\Delta T}{\Delta R} = \frac{-1}{\lambda_P + \sum_{i=1}^{N} \lambda^f_i} \quad (1)$$

Here λ_P is the Planck feedback parameter (−3.2 W m^{-2} K^{-1}) and λ^f_i (in W m^{-2} K^{-1}) represents the feedback parameters of any number (N) of fast (f) feedbacks. We define feedback parameters in the form $\lambda^f_i = \Delta R_i/\Delta T$. S^a is the 'Charney' sensitivity calculated by most climate models in '2 × CO_2' equilibrium simulations, with a range of 0.6–1.2 K W^{-1} m^2 in IPCC-AR4. However, the Earth system in reality responds to a perturbation according to an equilibrium climate sensitivity parameter S^p (where p indicates *palaeo*), but the timescales to reach this equilibrium are long, so that the forcing normally changes before equilibrium is reached. To obtain S^a from palaeoclimate sensitivity S^p, a correction is therefore needed for the slow feedback influences. Using λ^s_j to represent any number (M) of slow (s) feedbacks, we derive the general expression (see Supplementary Information):

$$S^a = S^p \left(1 + \frac{\sum_{j=1}^{M} \lambda_j^s}{\lambda_P + \sum_{i=1}^{N} \lambda_i^f} \right) \quad (2)$$

This approach is contingent on the above-mentioned caveats of state-dependence, linearization (small ΔT), changes in slow feedbacks, and transient effects, where the last is relevant only in records of exceptionally high temporal resolution. Knowledge of slow (λ^s) and fast (λ^f) feedbacks can be combined into a factor $F = \lambda^s/(\lambda^f + \lambda^s)$ that may then be used to back-calculate fast feedbacks out of palaeoclimate sensitivity S^p.

A recent study[44] defined the term 'Earth system sensitivity' (ESS) to represent the long-term climate response of Earth's climate system to a given CO_2 forcing, including both fast and slow processes. In our notation, ESS = $\Delta R_{2\times CO2}\ S^p$, where $\Delta R_{2\times CO2}$ is the forcing due to a CO_2-doubling (3.7 W m^{-2}).

Here we introduce a more explicit notation regarding what was (not) included in the climate sensitivity diagnosis. It is the 'specific climate sensitivity' $S_{[A,B...]}$, expressed in K W^{-1} m^2, where slow feedback processes A, B, and so on, are explicitly accounted for (that is, included in the forcing term, $\Delta R_{[A,B...]}$). We use 'LI' to denote albedo forcing due to land-ice volume/area changes, 'VG' for vegetation-albedo forcing, 'AE' for aerosol forcing and 'CO2' for atmospheric CO_2 forcing (see also Table 1). This approach requires from the outset that a comprehensive view is taken of the various causes of change in the radiative balance.

The most practical version of S to be estimated from palaeodata is $S_{[CO2,LI]}$, because $S_{[CO2,LI]} = S_{[CO2]}$ during times (pre-35 Myr ago) without ice volume, and because global vegetation cover changes, atmospheric dust fluctuations, and both CH_4 and N_2O fluctuations (the two important non-CO_2 GHGs) generally remain poorly constrained by proxy data. Common reporting of $S_{[CO2,LI]}$ would bring results closer in line with the model-based concept of 'equilibrium' fast-feedback sensitivity. The above-mentioned issues with aerosol influences mean that it would currently be best for estimates from palaeodata to report both $S_{[CO2,LI]}$ and $S_{[CO2,LI,AE]}$.

Table 2 lists example estimates for S following the main potential permutations of the definition of S in our approach (for detailed breakdowns, see Supplementary Information). The first example uses records of palaeodata since 800 kyr ago. The second example uses the same input data series[6], but focuses only on the LGM; the contrast between examples one and two thus highlights state-dependence. The third example lists estimates for $S_{[CO2]}$, $S_{[CO2,LI]}$ and $S_{[CO2,LI,VG]}$ from a more model-based assessment for the mid-Pliocene (~3–3.3 Myr ago)[13], with ΔT = 3.3 K relative to the present and ΔR_{CO2} = 1.9 W m^{-2} due to CO_2 increase from 280 to 400 parts per million by volume (p.p.m.v.; ref. 44). The broad range of S values found within each example illustrates that comparison across different definitions unrealistically widens the range of values reported, notably towards high values, because omission of 'forcing' due to the action of any slow feedbacks will cause overestimation of S (see also Fig. 3).

For a first-order estimate of the range of S from palaeodata that approximates compatibility with the centennial timescale 'equilibrium'

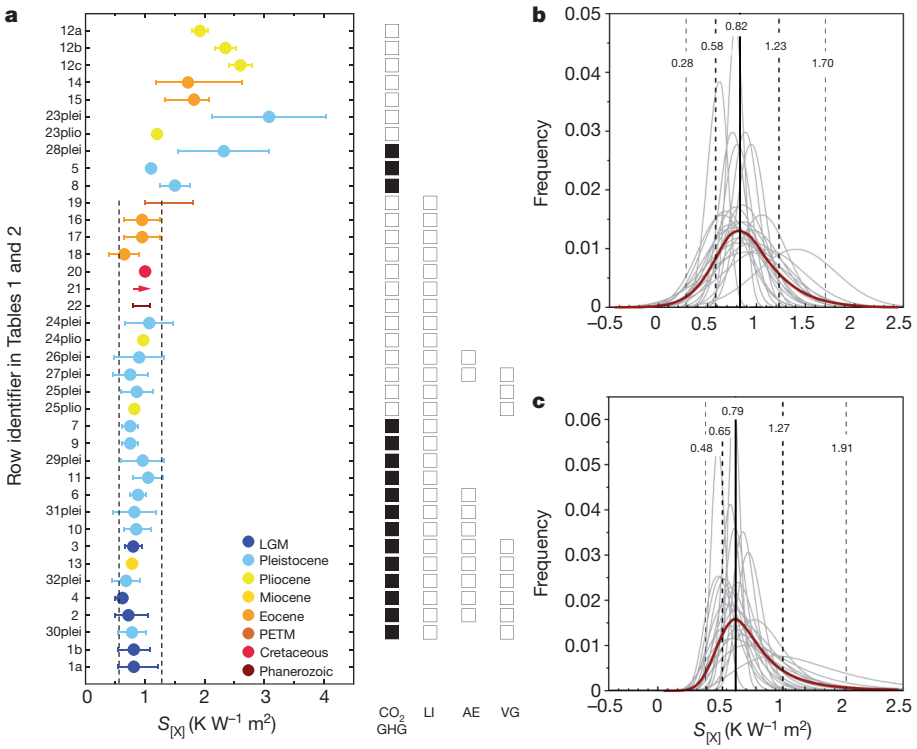

Figure 3 | Evaluation of results from Tables 1 and 2. *y*-Axis labels refer to numbered rows in these Tables. **a**, Data summary by table row. **b**, Probability assessment using normal distributions (shifted where relevant). **c**, Probability assessment using lognormal distributions. $S_{[X]}$ refers to the climate sensitivity as defined in detail by the subscript X in Tables 1 and 2. For **b** and **c**, we assume a relative uncertainty of 25% for entries that lacked uncertainty estimates in the source studies. In **a**, rows from Table 2 are identified with either 'plei' or 'plio' to distinguish between the past 800 kyr and the Pliocene entries, respectively. The colour coding refers to broad geological intervals, as shown in the key. Boxes at right indicate which conditions were explicitly accounted for; that is, as 'forcings' (in the CO_2/GHG column, filled squares indicate GHG and open squares CO_2). Circles (data points in **a**) show central values where reported, error bars represent uncertainties as outlined in the Tables, at the 1σ equivalent level. Arrow (case 21) indicates a value reported only as >0.8 K W^{-1} m^2. Black dashed lines in **a** show 68% probability limits for all estimates that account for at least 'CO2' and 'LI', based on thick dashed lines in **b** and **c**, taking whichever 68% value offers the widest (more conservatively estimated) margin. In **b** and **c**, the solid black line indicates the mode value (maximum), and the thin dashed lines the 95% probability limits. All distributions in **b** and **c** are given as individual normalized frequencies (grey lines), and as mean normalized frequencies (red line).

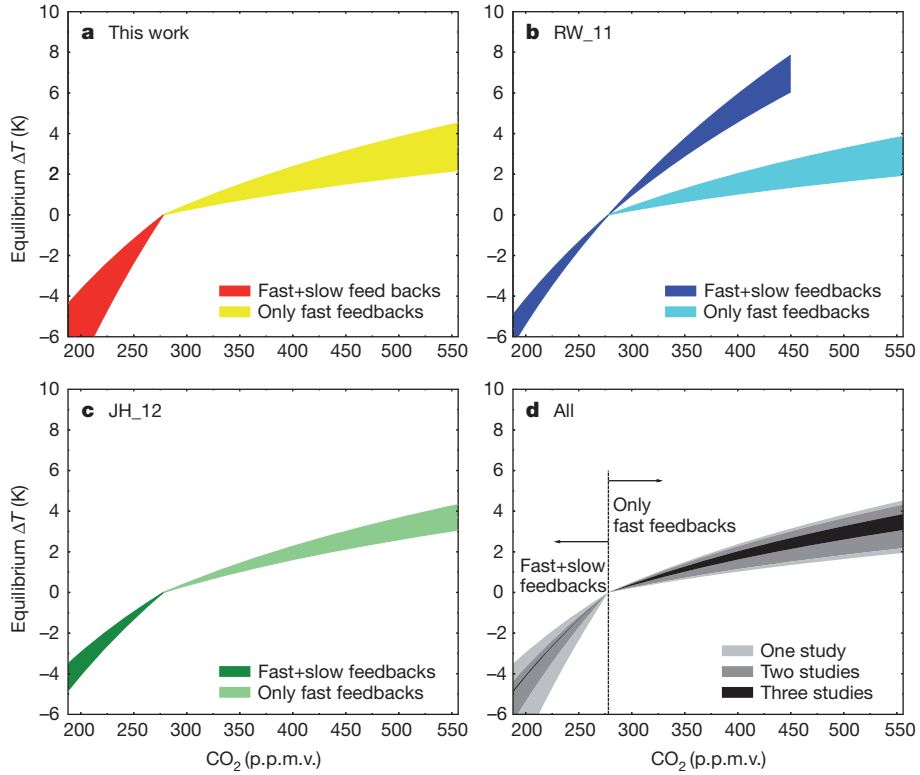

Figure 4 | Equilibrium response of the global temperature as a function of CO_2 concentrations, based on three different approaches. **a**, This work, using data from the late Pleistocene of the past 800 kyr (ref. 6). **b**, Using data of the past 20 Myr (RW_11; ref. 61). **c**, Based on JH_12 (ref. 85) using similar data of the past 800 kyr as in **a**. **d**, Combination of all three approaches. Plotted areas include uncertainty estimates of one standard deviation. Because this work and JH_12 developed their approach only on Pleistocene data (climate being mainly colder than today), extrapolation of the impact of slow feedbacks to $2 \times CO_2$ is not meaningful (we show only extrapolation with fast feedbacks). RW_11 in contrast also includes warmer climates with CO_2 up to 450 p.p.m.v., so that the applicable range with slow feedbacks extends to 450 p.p.m.v. For future climate with $2 \times CO_2$ and a short time horizon (<100 yr), only fast feedbacks are of interest (see **d**). Approaches partly disagree because of different assumptions. Uncertainties in this work (**a**) are estimated to be larger than they were in RW_11 (**b**) and JH_12 (**c**). For details of the equations and values used, see Supplementary Information.

values of the IPCC-AR4[1], values need to be used that account for 'CO_2' or 'GHG' as well as 'LI', and preferably also 'AE' and/or 'VG' (Tables 1, 2; Fig. 3). Such an assessment, excluding the case of row 21 in Table 1, yields a likely[1] (68%) probability range of 0.6–1.3 K W^{-1} m^2, and a 95% range of 0.3–1.9 K W^{-1} m^2 (Fig. 3). These represent the widest margins out of two assessments, using either normal distributions with shifts when relevant (Fig. 3a), or lognormal distributions that inherently allow asymmetry[2] (Fig. 3b). These assessments include uncertainties as outlined in the source studies, as well as any unaccounted-for dependence on different background climate states, but exclude potential additional uncertainties highlighted in this study. Inclusion of ESS values (approximated by $S_{[CO2]}$) would extend the upper limit beyond 3 K W^{-1} m^2 (Fig. 3a). Future work following a strict framework for reporting and comparison of palaeodata may refine the observed asymmetry.

Finally, following our conceptual framework, we can make a projection of equilibrium temperature change over a range of CO_2 concentrations while considering either slow and fast (or only fast) feedbacks (Fig. 4; see Supplementary Information for details). Including the known uncertainties associated with palaeoclimate sensitivity calculations, and comparing with two previous approaches[61,85], we find overlap in the 68% probability envelopes that implies equilibrium warming of 3.1–3.7 K for $2 \times CO_2$ (Fig. 4), equivalent to a fast feedback (Charney) climate sensitivity between 0.8 and 1.0 K W^{-1} m^2. For longer, multi-centennial projections, some of the slow feedbacks (namely vegetation-albedo and aerosol feedbacks) may need further consideration. However, their impact is difficult to estimate from palaeodata, because uncertainties are large, and because responses during climates colder than present may differ from responses during future warming.

We have employed a new framework of definitions for palaeoclimate sensitivity. This reveals how a broad selection of previously published estimates for the past 65 Myr agrees on a best general estimate of 0.6–1.3 K W^{-1} m^2, which agrees with IPCC-AR4 estimates for equilibrium climate sensitivity[1]. Higher estimates than ours may suggest different climate sensitivities during particular periods, but a considerable portion of the higher values may simply reflect differences in the definitions of palaeoclimate sensitivity that were used.

Received 18 April; accepted 11 September 2012.

1. Solomon, S. *et al.* (eds) *Climate Change 2007: The Physical Science Basis* (Cambridge Univ. Press, 2007).
2. Knutti, R. & Hegerl, G. C. The equilibrium sensitivity of the Earth's temperature to radiation changes. *Nature Geosci.* **1,** 735–743 (2008).
Presents a synthesis of equilibrium climate sensitivity estimates and discusses challenges for constraining its upper limit.
3. Houghton, J. T. *et al.* (eds) *Climate Change 2001: The Scientific Basis* (Cambridge Univ. Press, 2001).
4. Roe, G. H. Feedbacks, timescales and seeing red. *Annu. Rev. Earth Planet. Sci.* **37,** 93–115 (2009).
5. Dufresne, J.-L. & Bony, S. An assessment of the primary sources of spread of global warming estimates from coupled atmosphere-ocean models. *J. Clim.* **21,** 5135–5144 (2008).
Presents a compilation of results of 12 GCMs used in IPCC-AR4, on the contribution of different fast feedbacks to both equilibrium and transient temperature change.
6. Köhler, P. *et al.* What caused Earth's temperature variations during the last 800,000 years? Data-based evidences on radiative forcing and constraints on climate sensitivity. *Quat. Sci. Rev.* **29,** 129–145 (2010).
Presents a data compilation on radiative forcing over the past 800 kyr, which forms the backbone of our late Pleistocene examples in Table 2 and in Supplementary Information.
7. Roe, G. H. & Baker, M. B. Why is climate sensitivity so unpredictable? *Science* **318,** 629–632 (2007).

8. Baker, M. B. & Roe, G. H. The shape of things to come: why is climate change so predictable? *J. Clim.* **22,** 4574–4589 (2009).
9. Hannart, A., Dufresne, J.-L. & Naveau, P. Why climate sensitivity may not be so unpredictable. *Geophys. Res. Lett.* **36,** L16707 (2009).
10. Zaliapin, I. & Ghil, M. Another look at climate sensitivity. *Nonlinear Process. Geophys.* **17,** 113–122 (2010).
11. Colman, R. & McAvaney, B. Climate feedbacks under a very broad range of forcing. *Geophys. Res. Lett.* **36,** L01702 (2009).
12. Hargreaves, J. C., Abe-Ouchi, A. & Annan, J. D. Linking glacial and future climates through an ensemble of GCM simulations. *Clim. Past* **3,** 77–87 (2007).
13. Lunt, D. J. *et al.* On the causes of mid-Pliocene warmth and polar amplification. *Earth Planet. Sci. Lett.* **321–322,** 128–138 (2012).
14. Haywood, A. M. *et al.* Are there pre-Quaternary geological analogues for a future greenhouse warming? *Phil. Trans. R. Soc. A* **369,** 933–956 (2011).
15. Edwards, T. L., Crucifix, M. & Harrison, S. P. Using the past to constrain the future: how the palaeorecord can improve estimates of global warming. *Prog. Phys. Geogr.* **31,** 481–500 (2007).
16. Crucifix, M. Does the Last Glacial Maximum constrain climate sensitivity? *Geophys. Res. Lett.* **33,** L18701 (2006).
Presents first key evidence on the state-dependence of climate sensitivity.
17. Laîné, A., Kageyama, M., Braconnot, P. & Alkama, R. Impact of greenhouse gas concentration changes on the surface energetics in the IPSL-CM4 model: regional warming patterns, land/sea warming ratio, glacial/interglacial differences. *J. Clim.* **22,** 4621–4635 (2009).
18. Otto-Bliesner, B. L. Status of CCSM4 Paleo CMIP5 Climate Simulations. http://www.cesm.ucar.edu/events/ws.2011/Presentations/Paleo/bette.pdf.
19. Held, I. M. *et al.* Probing the fast and slow components of global warming by returning abruptly to preindustrial forcing. *J. Clim.* **23,** 2418–2427 (2010).
20. Joos, F. & Spahni, R. Rates of change in natural and anthropogenic radiative forcing over the past 20,000 years. *Proc. Natl Acad. Sci. USA* **105,** 1425–1430 (2008).
21. Köhler, P., Knorr, G., Buiron, D., Lourantou, A. & Chapellaz, J. Abrupt rise in atmospheric CO_2 at the onset of the Bølling/Allerød: in-situ ice core data versus true atmospheric signals. *Clim. Past* **7,** 473–486 (2011).
22. Hönisch, B. *et al.* The geological record of ocean acidification. *Science* **335,** 1058–1063 (2012).
23. Charney, J. G. *et al. Carbon Dioxide and Climate: A Scientific Assessment* (National Academy of Sciences, 1979).
24. Knutti, R. & Tomassini, L. Constraints on the transient climate response from observed global temperature and ocean heat uptake. *Geophys. Res. Lett.* **35,** L09701 (2008).
25. Gregory, J. M. & Forster, P. M. Transient climate response estimated from radiative forcing and observed temperature change. *J. Geophys. Res.* **113,** D23105 (2008).
26. Soden, B. J. & Held, I. M. An assessment of climate feedbacks in coupled ocean-atmosphere models. *J. Clim.* **19,** 3354–3360 (2006).
27. Huber, M., Mahlstein, I., Wild, M., Fasullo, J. & Knutti, R. Constraints on climate sensitivity from radiation patterns in climate models. *J. Clim.* **24,** 1034–1052 (2011).
28. Huybers, P. Compensation between model feedbacks and curtailment of climate sensitivity. *J. Clim.* **23,** 3009–3018 (2010).
29. Lemoine, D. M. Climate sensitivity distributions dependence on the possibility that models share biases. *J. Clim.* **23,** 4395–4415 (2010).
30. Hansen, J. Sato, M. Kharecha, P. & von Schuckmann, K. Earth's energy imbalance and implications. *Atmos. Chem. Phys.* **11,** 13421–13449 (2011).
31. Gregory, J. M. *et al.* A new method for diagnosing radiative forcing and climate sensitivity. *Geophys. Res. Lett.* **31,** L03205 (2004).
32. Lambert, F. *et al.* Dust-climate couplings over the past 800,000 years from the EPICA Dome C ice core. *Nature* **452,** 616–619 (2008).
33. Winckler, G., Anderson, R. F., Fleisher, M. Q., McGee, D. & Mahowald, N. Covariant glacial-interglacial dust fluxes in the equatorial Pacific and Antarctica. *Science* **320,** 93–96 (2008).
34. Roberts, A. P., Rohling, E. J., Grant, K. M., Larrasoaña, J. C. & Liu, Q. Atmospheric dust variability from major global source regions over the last 500,000 years. *Quat. Sci. Rev.* **30,** 3537–3541 (2011).
35. Ruth, U., Wagenbach, D., Steffensen, J. P. & Bigler, M. Continuous record of microparticle concentration and size distribution in the central Greenland NGRIP ice core during the last glacial period. *J. Geophys. Res.* **108,** 4098, http://dx.doi.org/10.1029/2002JD002376 (2003).
36. Naafs, B. D. A. *et al.* Strengthening of North American dust sources during the late Pliocene (2.7 Ma). *Earth Planet. Sci. Lett.* **317–318,** 8–19 (2012).
37. Kohfeld, K. E. & Harrison, S. P. DIRTMAP: the geological record of dust. *Earth Sci. Rev.* **54,** 81–114 (2001).
38. Mahowald, N., Albani, S., Engelstaedter, S., Winckler, G. & Goman, M. Model insight into glacial-interglacial paleodust records. *Quat. Sci. Rev.* **30,** 832–854 (2011).
39. Rohling, E. J., Medina-Elizalde, M., Shepherd, J. G., Siddall, M. & Stanford, J. D. Sea surface and high-latitude temperature sensitivity to radiative forcing of climate over several glacial cycles. *J. Clim.* **25,** 1635–1656 (2012).
40. Gray, L. J. *et al.* Solar influences on climate. *Rev. Geophys.* **48,** RG4001 (2010).
41. Milankovitch, M. *Kanon der Erdbestrahlung und seine Anwendung auf das Eiszeitenproblem* (Special Publication 133, Mathematics and Natural Sciences Section, Royal Serbian Academy, Belgrade, 1941).
42. Berger, A. Support for the astronomical theory of climatic change. *Nature* **269,** 44–45 (1977).
43. Laskar, J. *et al.* A long-term numerical solution for the insolation quantities of the Earth. *Astron. Astrophys.* **428,** 261–285 (2004).
44. Lunt, D. J. *et al.* Earth system sensitivity inferred from Pliocene modelling and data. *Nature Geosci.* **3,** 60–64 (2010).
Presents a definition of Earth system sensitivity that includes both fast and slow processes, and its application to the Pliocene.
45. Gregory, J. & Webb, M. Tropospheric adjustment induces a cloud component in CO_2 forcing. *J. Clim.* **21,** 58–71 (2008).
46. Lüthi, D. *et al.* High-resolution CO_2 concentration record 650,000–800,000 years before present. *Nature* **453,** 379–382 (2008).
47. Loulergue, L. *et al.* Orbital and millennial-scale features of atmospheric CH_4 over the past 800,000 years. *Nature* **453,** 383–386 (2008).
48. Schilt, A. *et al.* Glacial-interglacial and millennial-scale variations in the atmospheric nitrous oxide concentration during the last 800,000 years. *Quat. Sci. Rev.* **29,** 182–192 (2010).
49. Waelbroeck, C. *et al.* Sea-level and deep water temperature changes derived from benthic foraminifera isotopic records. *Quat. Sci. Rev.* **21,** 295–305 (2002).
50. Rohling, E. J. *et al.* Antarctic temperature and global sea level closely coupled over the past five glacial cycles. *Nature Geosci.* **2,** 500–504 (2009).
51. Bintanja, R., van de Wal, R. & Oerlemans, J. Modelled atmospheric temperatures and global sea levels over the past million years. *Nature* **437,** 125–128 (2005).
52. Hansen, J. *et al.* Target atmospheric CO_2: where should humanity aim? *Open Atmos. Sci. J.* **2,** 217–231 (2008).
53. Imbrie, J. & Imbrie, J. Z. Modeling the climatic response to orbital variations. *Science* **207,** 943–953 (1980).
54. Huybers, P. & Denton, G. H. Antarctic temperature at orbital timescales controlled by local summer duration. *Nature Geosci.* **1,** 787–792 (2008).
55. Huybers, P. Early Pleistocene glacial cycles and the integrated summer insolation forcing. *Science* **313,** 508–511 (2006).
56. Beerling, D. J. & Royer, D. L. Fossil plants as indicators of the Phanerozoic global carbon cycle. *Annu. Rev. Earth Planet. Sci.* **30,** 527–556 (2002).
57. Pagani, M., Zachos, J. C., Freeman, K. H., Tipple, B. & Bohaty, S. Marked decline in atmospheric carbon dioxide concentrations during the Paleogene. *Science* **309,** 600–603 (2005).
58. Hönisch, B., Hemming, N. G., Archer, D., Siddall, M. & McManus, J. F. Atmospheric carbon dioxide concentration across the mid-Pleistocene transition. *Science* **324,** 1551–1554 (2009).
59. Lowenstein, T. K. & Demicco, R. V. Elevated Eocene atmospheric CO_2 and its subsequent decline. *Science* **313,** 1928 (2006).
60. Beerling, D. J. & Royer, D. L. Convergent Cenozoic CO_2 history. *Nature Geosci.* **4,** 418–420 (2011).
61. van de Wal, R. S. W., de Boer, B., Lourens, L. J., Köhler, P. & Bintanja, R. Reconstruction of a continuous high-resolution CO_2 record over the past 20 million years. *Clim. Past* **7,** 1459–1469 (2011).
Compiles CO_2 data from a variety of approaches over the past 20 million years, and condenses these into one time series.
62. Beerling, D. J., Fox, A., Stevenson, D. S. & Valdes, P. J. Enhanced chemistry-climate feedbacks in past greenhouse worlds. *Proc. Natl Acad. Sci. USA* **108,** 9770–9775 (2011).
63. de Boer, B., van de Wal, R. S. W., Lourens, L. J. & Bintanja, R. Transient nature of the Earth's climate and the implications for the interpretation of benthic $\delta^{18}O$ records. *Palaeogeogr. Palaeoclimatol. Palaeoecol.* **335–336,** 4–11 (2011).
64. Cramer, B. S., Miller, K. G., Barrett, P. J. & Wright, J. D. Late Cretaceous-Neogene trends in deep ocean temperature and continental ice volume: reconciling records of benthic foraminiferal geochemistry ($\delta^{18}O$ and Mg/Ca) with sea level history. *J. Geophys. Res.* **116,** C12023 (2011).
65. Gasson, E. *et al.* Exploring uncertainties in the relationship between temperature, ice volume and sea level over the past 50 million years. *Rev. Geophys.* **50,** RG1005 (2012).
66. Zachos, J., Pagani, M., Sloan, L., Thomas, E. & Billups, K. Trends, rhythms, and aberrations in global climate 65 Ma to present. *Science* **292,** 686–693 (2001).
67. Miller, K. G., Wright, J. D. & Browning, J. V. Visions of ice sheets in a greenhouse world. *Mar. Geol.* **217,** 215–231 (2005).
68. Sluijs, A. *et al.* Eustatic variations during the Paleocene-Eocene greenhouse world. *Paleoceanography* **23,** PA4216 (2008).
69. Dickens, G. R., Castillo, M. M. & Walker, J. C. G. A blast of gas in the latest Paleocene: simulating first-order effects of massive dissociation of oceanic methane hydrate. *Geology* **25,** 259–262 (1997).
70. Lourens, L. J. *et al.* Astronomical pacing of late Palaeocene to early Eocene global warming events. *Nature* **435,** 1083–1087 (2005).
71. Zachos, J. C., Dickens, G. R. & Zeebe, R. E. An early Cenozoic perspective on greenhouse warming and carbon-cycle dynamics. *Nature* **451,** 279–283 (2008).
72. Zeebe, R. E., Zachos, J. C. & Dickens, G. R. Carbon dioxide forcing alone insufficient to explain Palaeocene-Eocene Thermal Maximum warming. *Nature Geosci.* **2,** 576–580 (2009).
73. Huber, M. & Caballero, R. The early Eocene equable climate problem revisited. *Clim. Past* **7,** 603–633 (2011).
74. Lorius, C., Jouzel, J., Raynaud, D., Hansen, J. & Le Treut, H. The ice-core record: climate sensitivity and future greenhouse warming. *Nature* **347,** 139–145 (1990).
75. Masson-Delmotte, V. *et al.* Past and future polar amplification of climate change: climate model intercomparisons and ice-core constraints. *Clim. Dyn.* **26,** 513–529 (2006).
76. Lea, D. The 100000-yr cycle in tropical SST, greenhouse gas forcing, and climate sensitivity. *J. Clim.* **17,** 2170–2179 (2004).
77. Hansen, J. *et al.* Climate change and trace gases. *Phil. Trans. R. Soc. Lond. A* **365,** 1925–1954 (2007).
78. Bijl, P. K. *et al.* Transient Middle Eocene atmospheric CO_2 and temperature variations. *Science* **330,** 819–821 (2010).
79. Schmittner, A. *et al.* Climate sensitivity estimated from temperature reconstructions of the Last Glacial Maximum. *Science* **334,** 1385–1388 (2011).
80. Rohling, E. J. Progress in palaeosalinity: overview and presentation of a new approach. *Paleoceanography* **22,** PA3215 (2007).

81. MARGO project members. Constraints on the magnitude and patterns of ocean cooling at the Last Glacial Maximum. *Nature Geosci.* **2,** 127–132 (2009).
82. Schneider von Deimling, T., Ganopolski, A., Held, H. & Rahmstorf, S. How cold was the Last Glacial Maximum? *Geophys. Res. Lett.* **33,** L14709 (2006).
83. Ballantyne, A. P., Lavine, M., Crowley, T. J., Liu, J. & Baker, P. B. Meta-analysis of tropical surface temperatures during the Last Glacial Maximum. *Geophys. Res. Lett.* **32,** L05712 (2005).
84. Hansen, J. *et al.* in *Climate Processes and Climate Sensitivity* (eds Hansen, J. & Takahashi, T.) 130–163 (Geophysical Monographs 29, American Geophysical Union, 1984).
85. Hansen, J. E. & Sato, M. in *Climate Change: Inferences from Paleoclimate and Regional Aspects* (eds Berger, A., Mesinger, F. & Šijački, D.) 21–48 (Springer, 2012).
86. Hoffert, M. I. & Covey, C. Deriving global climate sensitivity from palaeoclimate reconstructions. *Nature* **360,** 573–576 (1992).
87. Pagani, M., Liu, Z., LaRiviere, J. & Ravelo, A. C. High Earth-system climate sensitivity determined from Pliocene carbon dioxide concentrations. *Nature Geosci.* **3,** 27–30 (2010).
88. Covey, C., Sloan, L. C. & Hoffert, M. I. Paleoclimate data constraints on climate sensitivity: the paleocalibration method. *Clim. Change* **32,** 165–184 (1996).
89. Zachos, J. C., Stott, L. D. & Lohmann, K. C. Evolution of early Cenozoic marine temperatures. *Paleoceanography* **9,** 353–387 (1994).
90. Sloan, L. C. & Barron, E. J. A comparison of Eocene climate model results to quantified paleoclimatic interpretations. *Palaeogeogr. Palaeoclimatol. Palaeoecol.* **93,** 183–202 (1992).
91. Berner, R. A. A model for atmospheric CO_2 over Phanerozoic time. *Am. J. Sci.* **291,** 339–376 (1991).
92. Freeman, K. H. & Hayes, J. M. Fractionation of carbon isotopes by phytoplankton and estimates of ancient CO_2 levels. *Glob. Biogeochem. Cycles* **6,** 185–198 (1992).
93. Cerling, T. E. Carbon dioxide in the atmosphere; evidence from Cenozoic and Mesozoic paleosols. *Am. J. Sci.* **291,** 377–400 (1991).
94. Royer, D. L., Pagani, M. & Beerling, D. J. Geobiological constraints on Earth system sensitivity to CO_2 during the Cretaceous and Cenozoic. *Geobiology* **10,** 298–310 (2012).
95. Panchuk, K., Ridgwell, A. & Kump, L. R. Sedimentary response to Paleocene-Eocene Thermal Maximum carbon release: a model-data comparison. *Geology* **36,** 315–318 (2008).
96. Borzenkova, I. I. Determination of global climate sensitivity to the gas composition of the atmosphere from paleoclimatic data. *Izv. Atmos. Ocean. Phys.* **39,** 197–202 (2003).
97. Park, J. & Royer, D. L. Geologic constraints on the glacial amplification of Phanerozoic climate sensitivity. *Am. J. Sci.* **311,** 1–26 (2011).
98. Schmidt, G. A. Climate sensitivity — how sensitive is Earth's climate to CO_2; past. *PAGES News* **20,** 11 (2012).
99. Wunsch, C. & Heimbach, P. How long to oceanic tracer and proxy equilibrium? *Quat. Sci. Rev.* **27,** 637–651 (2008).

Supplementary Information is available in the online version of the paper.

Acknowledgements This Perspective arose from the first PALAEOSENS workshop in March 2011. We thank the Royal Netherlands Academy of Arts and Sciences (KNAW) for funding and hosting this workshop in Amsterdam, PAGES for their support, and J. Gregory for discussions. This study was supported by the UK-NERC consortium iGlass (NE/I009906/1), and 2012 Australian Laureate Fellowship FL120100050. D.J.B., E.J.R. and P.V. were supported by Royal Society Wolfson Research Merit Awards. A.S. thanks the European Research Council for ERC starting grant 259627, and M.H. acknowledges NSF P2C2 grant 0902882. Some of the work was supported by grant 243908 'Past4Future' of the EU's seventh framework programme; this is Past4Future contribution number 30.

Author Contributions E.J.R., A.S. and H.A.D. initiated the PALAEOSENS workshop, and led the drafting of this study together with P.K., A.S.v.d.H. and R.S.W.v.d.W. The other authors contributed specialist insights, discussions and feedback.

Author Information Reprints and permissions information is available at www.nature.com/reprints. The authors declare no competing financial interests. Readers are welcome to comment on the online version of the paper. Correspondence and requests for materials should be addressed to E.J.R. (e.rohling@noc.soton.ac.uk).

PALAEOSENS Project Members E. J. Rohling[1,2], A. Sluijs[3], H. A. Dijkstra[4], P. Köhler[5], R. S. W. van de Wal[4], A. S. von der Heydt[4], D. J. Beerling[6], A. Berger[7], P. K. Bijl[3], M. Crucifix[7], R. DeConto[8], S. S. Drijfhout[9], A. Fedorov[10], G. L. Foster[1], A. Ganopolski[11], J. Hansen[12], B. Hönisch[13], H. Hooghiemstra[14], M. Huber[15], P. Huybers[16], R. Knutti[17], D. W. Lea[18], L. J. Lourens[3], D. Lunt[19], V. Masson-Demotte[20], M. Medina-Elizalde[21], B. Otto-Bliesner[22], M. Pagani[10], H. Pälike[1,23], H. Renssen[24], D. L. Royer[25], M. Siddall[26], P. Valdes[19], J. C. Zachos[27] & R. E. Zeebe[28]

Affiliations for participants: [1]School of Ocean and Earth Science, University of Southampton, National Oceanography Centre, Southampton SO14 3ZH, UK. [2]Research School of Earth Sciences, The Australian National University, Canberra, Australian Capital Territory 0200, Australia. [3]Department of Earth Sciences, Faculty of Geosciences, Utrecht University, Budapestlaan 4, 3584 CD Utrecht, The Netherlands. [4]Institute for Marine and Atmospheric Research Utrecht, Utrecht University, 3584 CC Utrecht, The Netherlands. [5]Alfred Wegener Institute for Polar and Marine Research (AWI), PO Box 12 01 61, 27515 Bremerhaven, Germany. [6]Department of Animal and Plant Sciences, University of Sheffield, Sheffield S10 2TN, UK. [7]Georges Lemaitre Centre for Earth and Climate Research, Earth and Life Institute–Université catholique de Louvain, Chemin du Cyclotron 2, Box L7.01.11, 1348 Louvain-la-Neuve, Belgium. [8]Department of Geosciences, 611 North Pleasant Street, 233 Morrill Science Center, University of Massachusetts, Amherst, Massachusetts 01003-9297, USA. [9]Royal Netherlands Meteorological Institute, PO Box 201, 3730 AE De Bilt, The Netherlands. [10]Department of Geology and Geophysics, Yale University, PO Box 208109, New Haven, Connecticut 06520-8109, USA. [11]Potsdam Institute for Climate Impact Research (PIK), PO Box 601203, 14412 Potsdam, Germany. [12]NASA Goddard Institute for Space Studies, 2880 Broadway, New York, New York 10025, USA. [13]Lamont-Doherty Earth Observatory of Columbia University, Palisades, New York 10964, USA. [14]Institute for Biodiversity and Ecosystem Dynamics, University of Amsterdam, Science Park 904, 1098 XH Amsterdam, The Netherlands. [15]Earth and Atmospheric Sciences Department, Purdue University, West Lafayette, Indiana 47907, USA. [16]Department of Earth and Planetary Sciences, Harvard University, 20 Oxford Street, Cambridge, Massachusetts 02138, USA. [17]Institute for Atmospheric and Climate Science, ETH Zurich, Universitätstrasse 16, 8092 Zurich, Switzerland. [18]Department of Earth Science, University of California, Santa Barbara, California 93106-9630, USA. [19]School of Geographical Sciences, University of Bristol, University Road, Bristol BS8 1SS, UK. [20]LSCE (IPSL/CEA-CNRS-UVSQ), UMR 8212, LCEA Saclay, 91 191 Gif sur Yvette Cedex, France. [21]Centro de Investigación Científica de Yucatán, Unidad Ciencias del Agua, Cancún, Quintana Roo, 77500, México. [22]National Center for Atmospheric Research, PO Box 3000, Boulder, Colorado 80307-3000, USA. [23]MARUM, University of Bremen, Leobener Straße, 28359 Bremen, Germany. [24]Department of Earth Sciences, Faculty of Earth and Life Sciences, Free University Amsterdam, De Boelelaan 1085, NL1081HV Amsterdam, The Netherlands. [25]Department of Earth and Environmental Sciences, Wesleyan University, Middletown, Connecticut 06459, USA. [26]Department of Earth Sciences, University of Bristol, Wills Memorial Building, Queen's Road, Bristol BS8 1RJ, UK. [27]Earth and Planetary Sciences, University of California, Santa Cruz, California 95064, USA. [28]School of Ocean and Earth Science and Technology, Department of Oceanography, University of Hawaii at Manoa, 1000 Pope Road, MSB 629 Honolulu, Hawaii 96822, USA.